Journal of Catalysis 258 (2008) 95–102

Contents lists available at ScienceDirect

Journal of Catalysis

www.elsevier.com/locate/jcat

In situ FTIR study of the adsorption and reaction of *ortho*-dichlorobenzene on Pd–Co sulfated zirconia catalysts

Beatriz H. Aristizabal [a], Consuelo Montes de Correa [a,*], Alexander I. Serykh [b], Casey E. Hetrick [b], Michael D. Amiridis [b]

[a] *Environmental Catalysis Research Group, Universidad de Antioquia, A.A. 1226, Medellín, Colombia*
[b] *Department of Chemical Engineering, University of South Carolina, Columbia, SC 29208, USA*

ARTICLE INFO

Article history:
Received 17 December 2007
Revised 19 May 2008
Accepted 2 June 2008
Available online 3 July 2008

Keywords:
Oxidation
Adsorption
Ortho-dichlorobenzene
Sulfated zirconia
Cobalt
Palladium sulfated zirconia
FTIR

ABSTRACT

The adsorption and oxidation of *ortho*-dichlorobenzene (*o*-DCB) over sulfated zirconia (SZ), Co–SZ, and Pd/Co–SZ were studied by means of *in situ* FTIR spectroscopy to determine the nature of surface intermediates formed on these catalysts. The results indicate that *o*-DCB adsorbs on Lewis acid sites, forming surface intermediates that are strongly held on the surface. These intermediates can be subsequently oxidized to yield various partial oxidation products in either the presence or absence of gas-phase oxygen, confirming that surface oxygen is involved in the oxidation process. On Pd/Co–SZ samples, the oxidation is faster in the presence of gas-phase oxygen, yielding higher concentrations of partial oxidation products on the catalyst surface.

1. Introduction

The incineration of municipal, hazardous, and medical waste produces trace amounts of chlorinated volatile organic compounds (VOCs), including polychlorinated dibenzodioxins (PCDDs) and dibenzofurans (PCDFs). These are highly toxic, carcinogenic, and environmentally persistent organic pollutants (POPs). A stringent limit of 0.1 ng (TEQ)/Nm^3 (i.e., international toxicity equivalents per Nm^3) is in effect in several European countries and in Japan [1]. Among the technologies applied to destroy chlorinated organic compounds, catalytic oxidation is the preferred approach, due to its low destruction temperature and excellent selectivity toward formation of the desired products [2].

The catalytic oxidation of chlorinated aromatics is generally carried out over different catalysts, including noble metals (primarily Pt and Pd), perovskites, and transition metal oxides (i.e., Cu, Co, V, Mn, Fe, and Cr oxides) [2–5]. Noble metal and perovskite-based catalysts are highly active for the oxidation of chlorinated VOCs but may be susceptible to deactivation by the chlorine released during the reaction. Metal oxide catalysts appear to be more resistant to deactivation, but their catalytic activity is often lower. In general, the most commonly used catalytic systems for the oxidation of chlorinated VOCs are TiO_2-supported vanadia catalysts, frequently promoted to VO_x–WO_x/TiO_2 or VO_x–MoO_x/TiO_2 [2–7]. These catalysts were initially developed for the selective catalytic reduction of NO_x by NH_3 and also are known to be active in the oxidation of VOCs [5–7]. The effects of WO_x and MoO_x appear to be linked to the increased number of Brønsted acid sites on the catalyst surface [7,8].

Although limited information is available in the open literature regarding the use of ZrO_2-supported catalysts for the oxidation of chlorinated VOCs, the lability and ready exchangeability of oxygen atoms of the tetragonal phase make zirconia suitable for redox catalysis [9]. Moreover, ZrO_2 exhibits good mechanical properties and high thermal stability [10]. Zirconia doped with various oxoanions, such as sulfates, phosphates, and heteropolyanions, results in the stabilization of the tetragonal phase [10–15]. These surface oxoanions create additional electron-deficient regions that may generate new acid sites and increase the strength of Brønsted acidity [11,12]. Promoted sulfated zirconia catalysts also have been shown to maintain a highly dispersed active component and to have good hydrothermal stability [13,14].

In an attempt to develop new active and thermally stable catalysts for the destruction of persistent organic pollutants, in this work we report on the results of *in situ* infrared spectroscopic studies of *ortho*-dichlorobenzene (*o*-DCB) adsorption and oxidation over sulfated zirconia (SZ), Co–SZ, and Pd/Co–SZ catalysts. *o*-DCB, known to be an important precursor of PCDDs and PCDFs, is a suitable model compound for studying the catalytic oxidation of more

* Corresponding author.
E-mail address: cmontes@udea.edu.co (C. Montes de Correa).

0021-9517/$ – see front matter
doi:10.1016/j.jcat.2008.06.001

complex chlorinated POPs. Our goal is to gain more insight into the surface chemistry during these processes, as well as the roles of the different catalyst components.

2. Experimental

2.1. Catalyst preparation

Sulfated zirconia catalyst samples were prepared as reported previously [15]. In brief, 6.5 mL of zirconium butoxide [$Zr(OC_4H_9)_4$, Aldrich] was added to 22.5 mL of cyclohexane at 60 °C. The resulting solution (solution 1) was stirred for 1 h and then cooled at 3 °C. Then second solution of distilled water (4 mol/mol_{Zr}) and sulfuric acid (0.48 mol/mol_{Zr}) was added dropwise under continuous stirring, until the mixture became difficult to stir (approximately 1.3 mL added). After sulfation, the gel was aged for 24 h at room temperature without stirring, then dried at 70 °C and calcined in static air at 600 °C for 4 h. Co–SZ samples were prepared following the same procedure, but also adding a mixture of 0.2 g of cobalt acetate and 5.5 mL of ethanol to solution 1. Pd-containing catalysts were obtained by impregnating Co–SZ samples with an aqueous solution containing 0.0049 g of $Pd(NH_3)_4{\cdot}Cl_2{\cdot}H_2O$ per g of Co–SZ, to obtain a nominal Pd loading of approximately 0.2 wt%. After drying at 60 °C, the catalyst samples were heated for 4 h at 500 °C in flowing helium.

The elemental composition and surface areas of the synthesized materials are given in Table 1. Elemental analyses of Pd and Co were performed by atomic absorption spectroscopy (AAS). The sulfur content was determined from the weight loss between 500 and 800 °C by TGA using a 2950 TGA/HRV6 instrument. BET specific surface areas of previously degassed samples were calculated from nitrogen adsorption–desorption isotherms obtained with a Micromeritics Pulse Chemisorb 2700 analyzer. X-ray diffraction (XRD) patterns were collected in a Shimadzu XD-D1 diffractometer equipped with a Ni-filtered Cu$K\alpha$ radiation source (λ = 0.15418 nm) at 30 kV and 40 mA. Such XRD patterns of 2θ between 10° and 90° demonstrated that the tetragonal phase predominated in SZ, Co–SZ, and Pd/Co–SZ.

2.2. In situ FTIR studies

FTIR spectra were collected with a Nicolet 740 spectrometer equipped with a MCT-B detector cooled by liquid nitrogen. A homemade flow cell with a path length of 10 cm, capped at both ends by IR-transparent NaCl windows, was used for *in situ* measurements. The 30-mg samples were pressed into self-supported discs of approximately 1 cm diameter and placed in a sample holder at the center of the cell. The cell was heated externally, with the temperature measured by a thermocouple placed in close proximity to the catalyst sample. Transmission spectra were collected in the single-beam mode by recording 128 scans at a resolution of 4 cm^{-1}.

Before each experiment, catalyst samples were pretreated in flowing helium at 360 °C for 2 h. Depending on the experiment, the cell was cooled in flowing He either at room temperature or at 250 °C. Spectra of the clean catalyst surface were collected and used as the background. Adsorption studies were conducted by exposing catalyst samples to a stream of a flowing 500-ppm *o*-DCB/He mixture, obtained by passing helium through an *o*-DCB saturator. *In situ* FTIR spectra were collected at different time intervals until a steady state was reached. Finally, the cell was flushed with flowing He or a mixture of 8% O_2/He to determine the adsorption strength and the reactivity of the surface species formed. In some cases, the temperature also was increased to further evaluate the strength of adsorption. *In situ* FTIR experiments also were conducted with the full reaction mixture, comprising 500 ppm *o*-DCB and 8% O_2/He, flowing over catalyst samples.

Table 1
Sulfate and metal content, temperature of sulfate decomposition (T_d) and BET specific surface area of the synthesized catalysts

Catalyst	Wt% (TGA)		Wt% (AAS)		S_{BET} ($m^2\ g^{-1}$)
	SO_4^{2-}	T_d (°C)	Co	Pd	
SZ	7.2	730	–	–	58
Co–SZ	10.9	689	1.48	–	112
Pd/Co–SZ	9.8	680	1.51	0.21	100

3. Results and discussion

3.1. o-DCB adsorption and reaction on ZrO_2 and SZ

FTIR spectra collected at different time intervals during *o*-DCB adsorption onto commercial ZrO_2 at room temperature exhibited bands at 1689, 1573, 1458, 1435, 1374, and 1248 cm^{-1} (Fig. 1, traces a and b). The bands at 1573, 1458, and 1435 cm^{-1} can be assigned to the C·⚊·C degenerate stretching vibrations of the aromatic ring [16]. The bands at 1573 and 1458 cm^{-1} were shifted slightly from the 1588 and 1461 cm^{-1} positions seen for gas-phase *o*-DCB (not shown). In a similar example of chlorobenzene adsorption on TiO_2 [17], the gas-phase band at 1588 cm^{-1} was shifted to 1582 cm^{-1} after, an effect attributed to the formation of a π-complex between surface Ti^{4+} ions and the aromatic ring. It was further proposed that such a complex was formed on a dehydroxylated surface, while a dual-site interaction (i.e., OH···π-electron and OH···Cl) occurred on surfaces with high hydroxyl group concentrations [17]. A similar mechanism can be proposed for *o*-DCB adsorption on commercial ZrO_2.

The intensities of the three bands at 1573, 1458, and 1435 cm^{-1} decreased after 60 min in flowing He at room temperature, demonstrating the adsorbed species' low stability. In contrast, the intensities of the bands at 1689 and 1374 cm^{-1} did not decrease in flowing He (Fig. 1, trace c), suggesting the presence of two different adsorbed species. The undissociated *o*-DCB molecules in

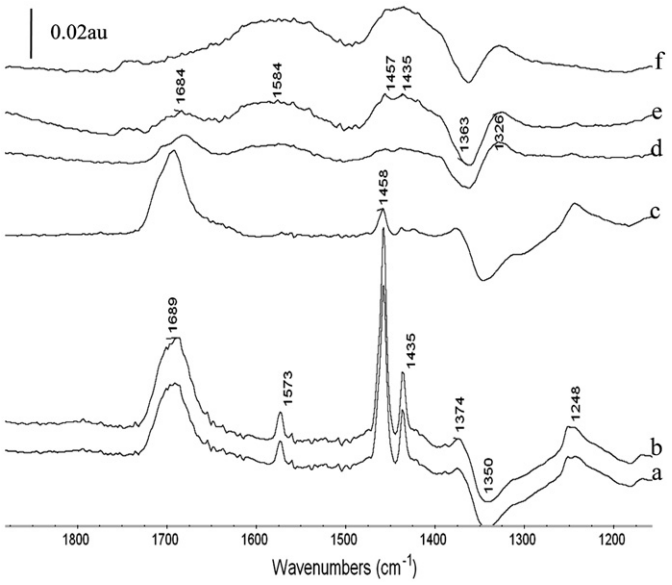

Fig. 1. *In situ* FTIR spectra of a commercial ZrO_2 sample collected at room temperature after (a) 10 min, (b) 120 min, in a stream of 500 ppm *o*-DCB/He, (c) 60 min of subsequent exposure to flowing He; at 250 °C after (d) 10 min, (e) 120 min, in a stream of 500 ppm *o*-DCB/He, (f) after 60 min of subsequent exposure to flowing He.

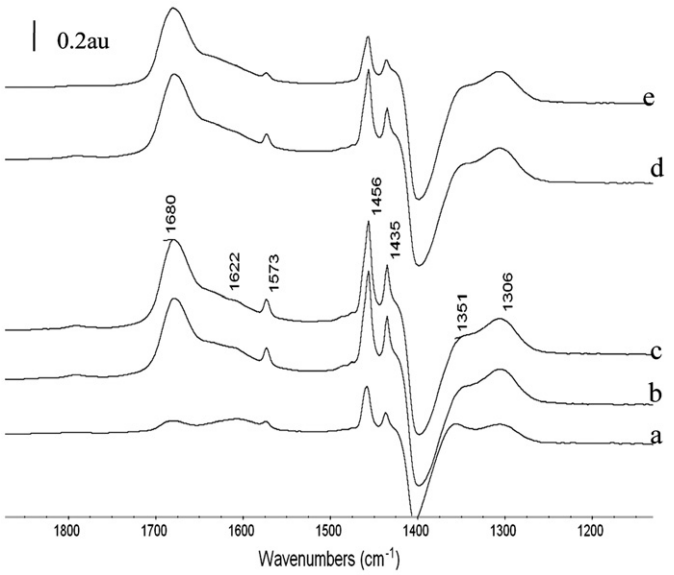

Fig. 2. *In situ* FTIR spectra of a SZ sample collected at room temperature after (a) 3 min, (b) 60 min, (c) 120 min, in a stream of 500 ppm *o*-DCB/He, and (d) after 20 min, (e) 60 min, of subsequent exposure to flowing He.

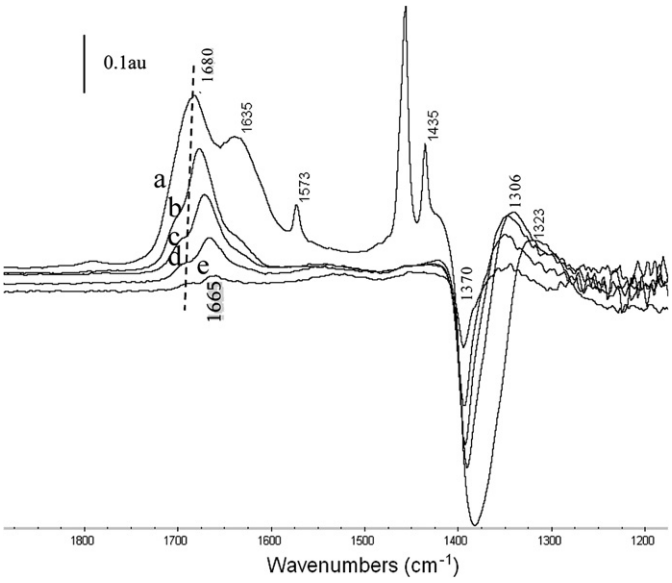

Fig. 3. *In situ* FTIR spectra of a SZ sample collected at room temperature after 120 min in a stream of 500 ppm *o*-DCB/He and 60 min of subsequent exposure to flowing He at: (a) room temperature, (b) 200 °C, (c) 250 °C, (d) 300 °C, and (e) 350 °C.

addition to the π bonding likely are further stabilized via hydrogen bonding, whereas the presence of surface oxygen in the form of O^{2-} ions, O^{2-} clusters, and residual hydroxyl groups may be responsible for acid–base-type interactions yielding the second species [18,19]. Dai et al. [19] found that halomethanes (CF_3Cl, CF_2Cl_2, $CFCl_3$, and CCl_4) react on γ-alumina surfaces at low temperatures through C–X (X = F, Cl) bond rupture. This process most likely is initiated by the formation of Al–X bonds on the alumina surface, with the resulting species (CX_{n-1}), which are electropositive, binding further to surface oxygen (O^{2-}, OH^-). In our case, the bands at 1689 and 1374 cm^{-1} can be assigned to vibrations of *o*-DCB adsorbed on Lewis acid sites of ZrO_2 following chlorine substraction by nucleophilic oxygen. This species is strongly bonded on the surface and can sustain the He flushing step.

Finally, a negative band at 1350 cm^{-1} and the remaining positive band at 1248 cm^{-1} are associated with the displacement of surface carbonate and bicarbonate species that were not completely eliminated during catalyst pretreatment at 360 °C. Such residual species often are observed on zirconia surfaces and cannot be removed by high-temperature activation [20]. Nevertheless, it appears that *o*-DCB adsorption caused a perturbation of these residual carbonate species.

When the *o*-DCB adsorption was conducted at 250 °C (Fig. 1, traces d and e), broader bands were observed at 1684, 1584, 1457, and 1435 cm^{-1}. The spectral changes shown in Fig. 1 (traces d and e) clearly indicate that at this temperature *o*-DCB reacts with ZrO_2 surface oxygen forming partial oxidation products, primarily carboxylates of the acetate type (νCOO^- sym and νCOO^- asym at 1457 and 1584 cm^{-1}) [5]. A weak feature at 1435 cm^{-1} (νCOO^- sym) also suggests the formation of surface formate species [5,21,22]. It has been reported that pure ZrO_2 can catalyze different reactions [23]. The adsorption of *o*-DCB at 250 °C demonstrated its oxidation ability. Furthermore, adsorbed species at 250 °C resisted He treatment at the same temperature, suggesting moderate stability (Fig. 1, trace f). The negative and positive bands from perturbed carbonate species were shifted to higher frequencies (1363 and 1326 cm^{-1}) at 250 °C, indicating weaker perturbation due to *o*-DCB. As a result, the 1374 cm^{-1} band observed at room temperature was not seen at 250 °C, due to overlapping with the shifted carbonate bands.

Spectra of the hydroxyl region (not shown) suggest that the adsorption of *o*-DCB affected the ZrO_2 surface hydroxyl groups at room temperature, whereas only a very weak perturbation was observed at 250 °C. The room temperature spectra exhibited negative bands in the 3750–3650 cm^{-1} range, which usually are assigned to strong surface hydroxyl groups, along with a broad positive band between 3650 and 3550 cm^{-1} (centered at approximately 3608 cm^{-1}). These spectra suggest that the strong ZrO_2 surface hydroxyls interact with *o*-DCB molecules during adsorption, leading to the formation of weaker hydrogen-bonded OHs [24,25].

Fig. 2 shows spectra of *o*-DCB adsorbed on SZ at room temperature. The spectra show well-defined bands at 1680, 1573, 1456, 1435, and 1306 cm^{-1}. A shoulder at 1622 cm^{-1} can be assigned to adsorbed water on the surface. The same *o*-DCB bands discussed previously for ZrO_2 appeared on introducing of the 500 ppm *o*-DCB/He stream (Fig. 2, traces a–c). Subsequent He flushing at room temperature (Fig. 2, traces d and e) resulted in decreased intensity of the bands at 1573, 1456, and 1435 cm^{-1}, consistent with the assignment of these bands to a weakly adsorbed *o*-DCB species (i.e., physisorption). But the intensity of the 1680 cm^{-1} band remained almost constant even after the temperature was raised to 300 °C (Fig. 3, trace d), indicating that the species corresponding to this band was strongly adsorbed on the surface. In addition, during desorption at high temperature, a shift toward lower wavenumbers occurred (i.e., a red shift of 15 cm^{-1} from room temperature to 350 °C), which can be attributed to the decreased *o*-DCB surface coverage at high temperatures, in agreement with a previous report [26].

Perturbation of surface sulfate is known to result in a negative band at approximately 1350–1400 cm^{-1} and a positive band at approximately 1300 cm^{-1} [20]. Indeed, the negative band at 1370–1390 cm^{-1} and the positive band at 1306 cm^{-1} in the spectra of Figs. 2 and 3 indicate the involvement of sulfate groups in the adsorption of *o*-DCB. The intensities of these bands were reduced when the adsorbed *o*-DCB was removed from the surface at high temperatures (Fig. 3, trace e). This result indicates that the perturbation of the sulfate groups was caused primarily by the adsorbed *o*-DCB species associated with the band at 1680 cm^{-1}. Furthermore, the adsorption on the sulfate groups appears to be mostly reversible.

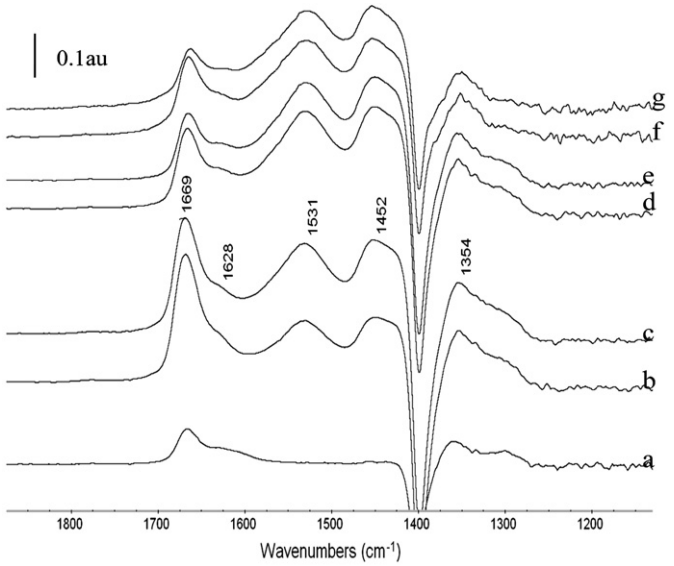

Fig. 4. *In situ* FTIR spectra of a SZ sample collected at 250 °C after (a) 3 min, (b) 60 min, (c) 120 min in a stream of 500 ppm *o*-DCB/He; after (d) 20 min, (e) 60 min of subsequent exposure to flowing He; and after (f) 20 min, (g) 60 min of subsequent exposure to a flowing 8% O_2/He mixture.

Spectra collected after the adsorption of *o*-DCB on SZ at 250 °C are shown in Fig. 4 (traces a–c). Under these conditions, the strong band seen at 1680 cm^{-1}at room temperature was shifted to 1669 cm^{-1}. Once again, a small shoulder at 1628 cm^{-1} occurred, attributed to the presence of some residual water. In addition, two new, broader bands were seen at 1531 and 1452 cm^{-1}. The band at 1669 cm^{-1} appeared immediately after the introduction of *o*-DCB, reached a maximum after 40 min on stream, and then decreased in intensity thereafter. The bands at 1531 and 1452 cm^{-1} became visible after 20 min on stream, and they continued to increase in intensity even as the intensity of the 1669 cm^{-1} band decreased. The negative and positive bands assigned earlier to perturbation of the sulfate groups were shifted to 1400 and 1354 cm^{-1}.

It is interesting to note that the band at 1669 cm^{-1} was not present in the spectra of *o*-DCB adsorbed on H-MOR samples, which contained only Brønsted acid sites [25]; however, a similar band was observed on adsorption of *o*-DCB on Co-MOR containing Co^{2+} Lewis acid sites [25]. The bands observed at 1684 cm^{-1} on ZrO_2, 1680 cm^{-1} on SZ at room temperature, and 1669 cm^{-1} on SZ at 250 °C suggest the presence of the same surface *o*-DCB species in all cases. We propose that this species was coordinated on the Lewis acid sites of ZrO_2 and SZ, possibly after chlorine abstraction by nucleophilic oxygen [19]. The specific band corresponds to the C=C stretching vibrations of the aromatic ring coordinated to the Lewis acid sites. This species can further react and form partial oxidation products [16,25].

Larrubia and Busca [16] have proposed that *o*-DCB reversibly adsorbs on V_2O_5–MoO_3–TiO_2 through its chlorine atoms and that irreversible reaction occurs through a concerted mechanism involving the interaction of a chlorine atom of the adsorbed molecules with a Lewis acid site located near an oxide or hydroxide nucleophilic site (i.e., nucleophilic substitution of the chlorine atom). According to Dai et al. [19], Al^{3+} sites are crucial for the dissociative chemisorption of CF_2Cl_2 and other halomethanes on γ-alumina. Coordinatively unsaturated Al^{3+} ions as well as O^{2-} ions act as Lewis acids and bases, respectively. Thus, the dissociative chemisorption process is initiated with the formation of Al–X bonds on the alumina surface. Furthermore, the electropositive fragment binds to O^{2-} species and/or residual hydroxyl groups, forming a C–O bond [19]. The importance of the surface acid–base properties also was in evidence during the adsorption and reaction of acetone on different oxides, including Al_2O_3, TiO_2, ZrO_2, and CeO_2 [27]. Dai et al. [19] pointed out that Lewis acid and base sites generate pairs of particularly strong adsorption capacity toward condensation products. The interactions of acetone and oxide interfaces lead to coordination of acetone molecules to Lewis acid sites [$(CH_3)_2C{=}O \rightarrow M^{n+}$] and to the presence of basic sites (surface–OH^- or $-O^{2-}$ site) in close proximity. Consequently, anionic enolate type ions are formed [$CH_2(CH_3)C{-}O^- \rightarrow M^{n+}$]. Basic sites are considered to play a key role in such oxidative reactions [5,19,27]; however, the availability of Lewis acid sites is essential for the formation of primary species, such as *o*-DCB–L [16], Al–X [19], and Ac–L [27].

Previous investigations have proposed that the first step in the catalytic oxidation of chlorinated benzenes over V_2O_5/TiO_2 catalysts is a nucleophilic substitution [5]. During the nucleophilic substitution (by O^{2-} ions), the chlorine atom is abstracted and replaced by a surface oxygen species, forming surface phenolates. Accordingly, Larrubia et al. [16] and Dai et al. [19] reported that the dissociative chemisorption process is most likely initiated by formation of the primary L → X species. But the type of Lewis and base sites present can affect the strength of the interaction and the type of the surface species formed; thus, the most dominant species depends on the nature of the oxide surface. For example, Zaki et al. [27] observed that during the reaction of acetone on Al_2O_3, TiO_2, ZrO_2, and CeO_2, the formation of primary species (coordinated acetone on Lewis sites, Ac → L) was the dominant species on a ZrO_2 surface (Ac → Zr^{4+}). This type of species is stabilized on surfaces that are essentially acidic and do not contain strong Lewis basic sites. On the other hand, the availability of strong basic sites is important for further conversion of the Ac → L species into condensation products.

Bands in the 1530–1580 and 1435–1460 cm^{-1} range have been assigned to carboxylate species of the acetate type [5,21]. Chintawar and Greene [21] for example, observed the presence of intense and well-defined bands at 1568 and 1445 cm^{-1} after the adsorption of trichloroethylene on a Cr–Y sample and assigned them to the COO^- asymmetric and symmetric stretching vibrations of surface acetates, respectively. They also reported changes in the frequency of these vibrations with the chlorine content of the feed molecule. More specifically, blue and red shifts were observed in the COO^- (asym) and COO^- (sym) frequencies, respectively, with increasing chlorine content. In agreement with these observations, we assigned the bands at 1531 and 1452 cm^{-1} to the COO^- vibrations of surface acetates. The oxidation process toward these products is initiated even in the absence of gas-phase oxygen, with surface ZrO_2 oxygen likely involved in the reaction, in agreement with previous reports [5,24].

Exposure of the surface species formed to flowing He (Fig. 4, traces d and e) did not result in any significant change in the intensities of the acetate bands at 1531 and 1452 cm^{-1}, indicating these bands' relatively high stability on the catalyst surface. In contrast, the intensity of the band at 1669 cm^{-1} decreased slowly in flowing He and faster in the presence of gas-phase oxygen (Fig. 4, traces f and g). These results suggest that the species characterized by this band could be a reactive intermediate.

When SZ was exposed to the complete reaction mixture (500 ppm *o*-DCB and 8% O_2/He), bands at 1666, 1536 and 1453 cm^{-1} were observed (Fig. 5, traces a–e). It is important to note that the intensities of the surface acetate bands were more pronounced in the presence of gas-phase oxygen. When present, gas-phase oxygen replenishes the catalyst surface, thereby enhancing the rate of formation of partial oxidation products.

In the OH region, positive and negative bands were seen at 3678 and 3648 cm^{-1} at room temperature, shifting to 3664 and 3633 cm^{-1} at 250 °C. A broad asymmetric band with a maximum at approximately 3548 cm^{-1} also was seen. Stevens et al. [28]

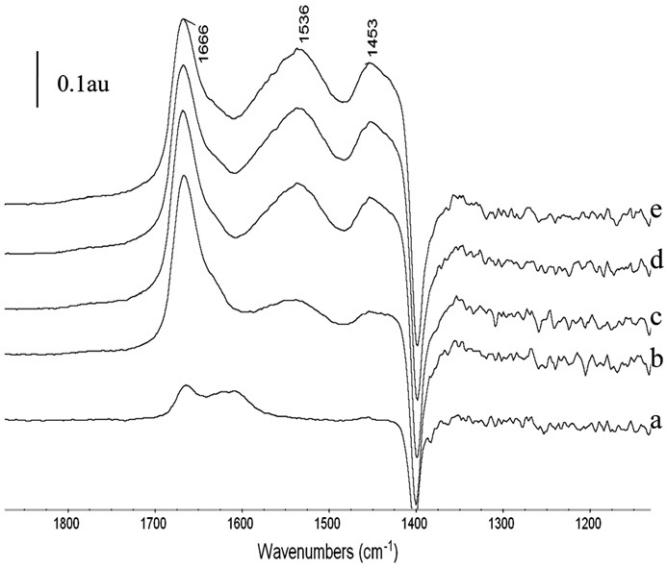

Fig. 5. *In situ* FTIR spectra of a SZ sample collected at 250 °C after (a) 3 min, (b) 20 min, (c) 60 min, (d) 80 min, and (e) 120 min in a stream of 500 ppm *o*-DCB/8% O_2/balance He.

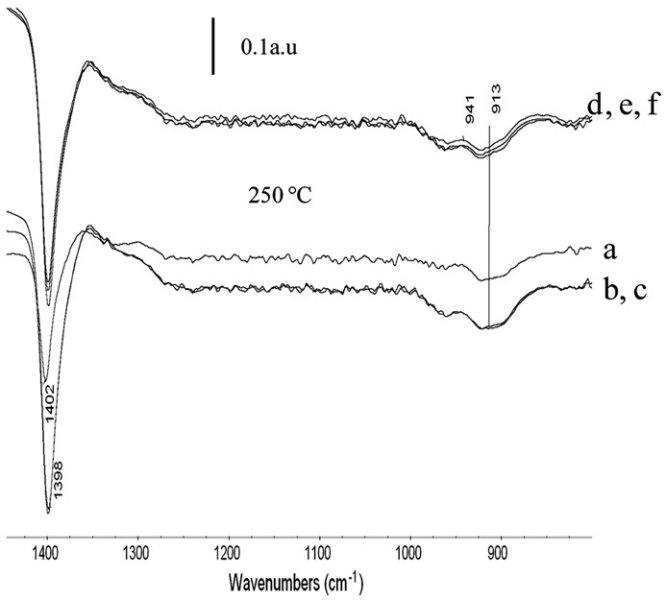

Fig. 6. *In situ* FTIR spectra of a SZ sample collected at 250 °C after (a) 3 min, (b) 40 min, (c) 60 min in a stream of 500 ppm *o*-DCB/He and after (d) 10 min, (e) 40 min, and (f) 60 min of subsequent exposure of the adsorbed species to flowing He.

assigned a band seen at 3678 cm^{-1} to the formation of bridged hydroxyls on sulfated zirconia (i.e., –OH groups bound to two zirconium atoms), and a negative band at 3648 cm^{-1} to the loss of terminal S–OH groups. The relatively low frequency shifts seen can be attributed to the effect of temperature [28]. Furthermore, broad bands in the 3500–3600 cm^{-1} range have been previously assigned to strongly hydrogen-bonded OH groups [29].

Different groups have reported that the adsorption of molecules such as NO on sulfated zirconia leads to the perturbation of the sulfate groups [15,20]. This perturbation is characterized by a negative band in the 1430–1300 cm^{-1} region assigned to the S=O stretching vibrations of the surface sulfate groups [30]. More specifically, surface sulfates of high covalence are characterized by a $\nu_{S=O}$ mode at wave numbers above 1390 cm^{-1} [30]. The concentration of sulfates and the degree of hydration of the surface are important parameters affecting the nature and strength of acidic centers in sulfated zirconia (SZ) [31]. Various groups [30,32,33] have reported that polynuclear complexes of the $[(Zr–O)_2(SO)]_2–O$ type ($\nu_{S=O} \geqslant 1400$ cm^{-1}) are formed at high sulfate loadings, with one coupled S–O–S bridge and two isolated S=O oscillators [32]. It has been further postulated that such S=O oscillators are bonded to the oxide network by S–O–Zr bridges. The IR spectra of the SZ catalysts collected in the present study exhibited two groups of negative bands in the 900–950 cm^{-1} range and another one at approximately 1400 cm^{-1} (Fig. 6). The weak negative bands in the 900–950 cm^{-1} region can be assigned to the interaction of adsorbed molecules with bridging S–O bonds [32]. In contrast, the sharp negative band at 1400 cm^{-1} can be assigned to the strong interaction of *o*-DCB with the S=O groups [28]. Alternatively, the possibility exists that *o*-DCB may not adsorb on the sulfate groups, but rather some oxygen atoms of the surface sulfates react with adsorbed *o*-DCB to yield partial oxidation products. When *o*-DCB was removed from the surface in flowing He, the intensity of the S=O band became less negative, indicating restoration of some of the S=O sites. At the same time, a shift of the S=O stretching vibration occurred toward lower frequencies, related to electron withdrawal by adsorbed molecules [34]. The negative band was almost completely restored in the presence of O_2 (Fig. 4). These results suggest that both *o*-DCB adsorption and reaction occurred on the surface sulfate groups, which can replenish their S=O sites by gas-phase oxygen, thus completing a catalytic cycle.

The Lewis and Brønsted acid sites present on SZ have been studied extensively [28–30,32,35]. Some authors [31] have attributed the strong Brønsted acidity of sulfated zirconia to surface hydroxyl groups, with the proton-donating ability of such groups enhanced by the electron-inductive effect of S=O. Others [32] have posited that the polynuclear complexes formed on extended patches of regular crystal planes can induce protonic acid activity, which is strictly determined by the degree of surface hydration. Lewis acid sites on sulfated zirconia have been associated with coordinatively unsaturated Zr^{4+} centers located in crystalographically defective configurations and on low-index crystal planes [32]. In addition, it has been reported that pyrosulfate is a possible stable structure on the tetragonal zirconia (101) face [35] and can generate greater numbers of Zr coordinative bonds (with weaker Zr–O bond strength), thereby facilitating the formation of Lewis sites and nearby Brønsted S–OH sites [33]. Consistent with these previous observations, we suggest that in our SZ materials, surface sulfates may have been combined with Zr in the bridging bidentated state to create strong acidity, with both Brønsted and nearby Lewis acid sites present. Both sites can participate in the reaction through a concerted mechanism involving Lewis acid sites and oxide and hydroxide-nucleophilic species [16,19]. During nucleophilic substitution, one of the chlorine atoms is abstracted and replaced by a surface oxygen species [5,16]; thus, hydroxyl groups and O^{2-} of the support can actively participate. The IR spectra exhibited differences between the ZrO_2 and SZ materials. The presence of sulfate groups on the ZrO_2 surface modified the catalyst surface active centers, yielding basic sites and promoting reaction of the coordinated species on the Lewis acid sites (*o*-DCB → L) toward partial oxidation products.

3.2. *o*-DCB adsorption and reaction on Co–SZ and Pd/Co–SZ

The spectra collected during the adsorption of *o*-DCB on Co–SZ at 250 °C (Fig. 7, traces a–c) were similar to those obtained with SZ. Once again, the bands 1668 and 1352 cm^{-1} appeared after the 500-ppm *o*-DCB/He mixture was introduced into the Co–SZ sample. This finding suggests that the adsorption of *o*-DCB on Co–SZ proceeded on similar Lewis acid sites on SZ. The acetate bands at

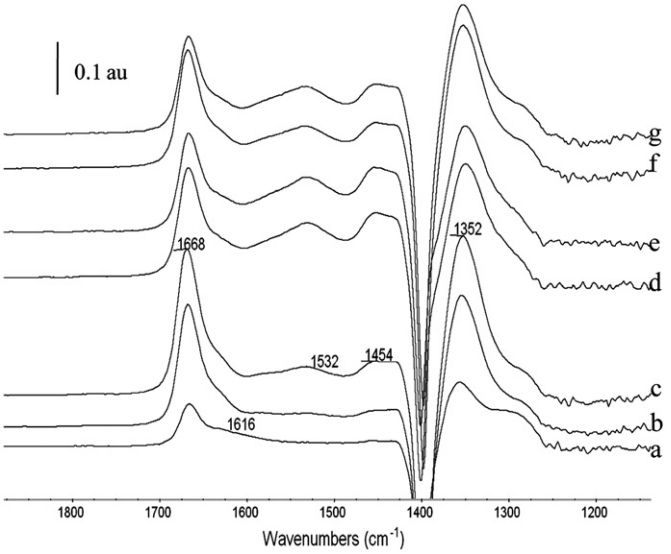

Fig. 7. *In situ* FTIR spectra of a Co–SZ sample collected at 250 °C after (a) 3 min, (b) 60 min, (c) 120 min in a stream of 500 ppm *o*-DCB/He; after (d) 20 min, (e) 60 min of subsequent exposure to flowing He; and after (f) 20 min, (g) 60 min of subsequent exposure to a flowing 8% O_2/He mixture.

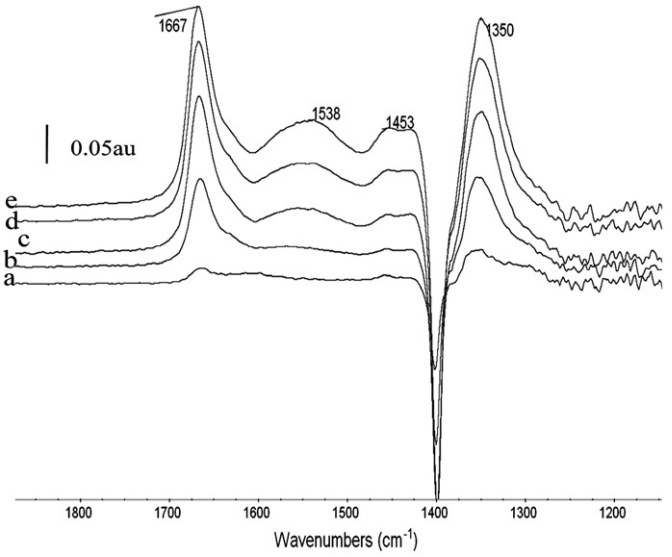

Fig. 8. *In situ* FTIR spectra of a Co–SZ sample collected at 250 °C after (a) 3 min, (b) 20 min, (c) 60 min, (d) 80 min, (e) 120 min in a stream of 500 ppm *o*-DCB/ 8% O_2/balance He.

1532 and 1454 cm^{-1} (Fig. 7, trace c) assigned to surface acetates were of weaker intensity than those seen on SZ. Finally, the shoulder observed at 1616 cm^{-1} (Fig. 7, trace a) once again suggests the presence of some residual water in the fresh sample. Spectra collected at the same temperature after the removal of *o*-DCB from the gas phase and flushing of the cell with either He (Fig. 7, traces d and e) or 8% O_2/He (Fig. 7, traces f and g) demonstrate that the intensity of the 1668 cm^{-1} band decreased, while the other bands remained rather stable. Similar bands also were seen when the Co–SZ catalyst was exposed to the complete reaction mixture (Fig. 8). The intensity of acetate bands increased in this case, indicating that gas-phase oxygen enhanced the formation of these species. All sets of spectra also contained a negative feature at approximately 1400 cm^{-1} that can be assigned to perturbation of the surface S=O groups of Co–SZ, similar to that discussed earlier for the SZ samples.

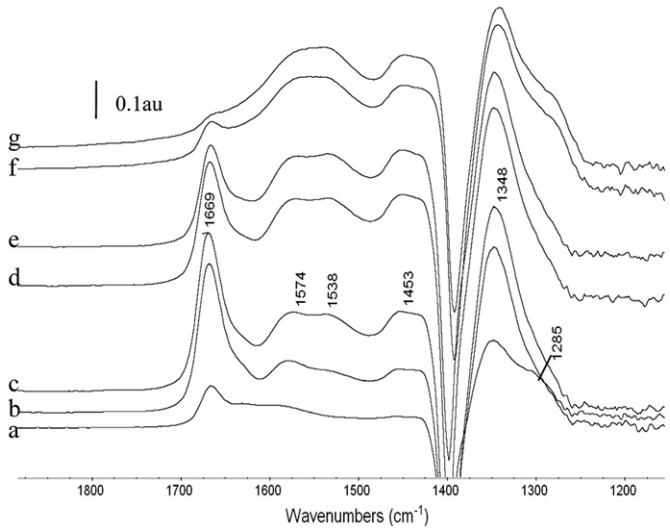

Fig. 9. *In situ* FTIR spectra of a Pd/Co–SZ sample collected at 250 °C after (a) 3 min, (b) 60 min, (c) 120 min in a stream of 500 ppm *o*-DCB/He; after (d) 20 min, (e) 60 min of subsequent exposure to flowing He; after (f) 20 min, (g) 60 min of subsequent exposure to a flowing 8% O_2/He mixture.

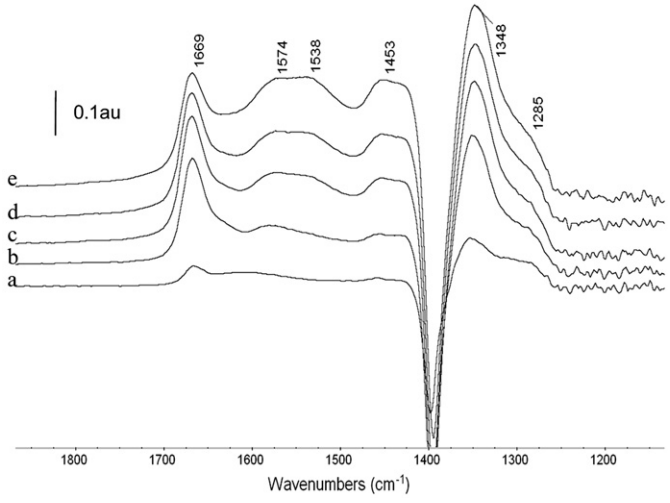

Fig. 10. *In situ* FTIR spectra of a Pd/Co–SZ sample collected at 250 °C after (a) 3 min, (b) 20 min, (c) 60 min, (d) 80 min, (e) 120 min in a stream of 500 ppm *o*-DCB/ 8% O_2/balance He.

The lower intensity of the acetate bands, and thus the lower concentration of surface acetates in the absence of gas-phase oxygen, may indicate decreased availability of reactive surface oxygen (i.e., S–OH or S=O) in the Co–SZ samples. This hypothesis is further supported by the absence of any strong features associated with the S–OH species in the hydroxyl region. Most likely, this resulted from the presence of the cobalt precursor during the gelation step, which is known to result in the formation of very stable species between cobalt and sulfate [36], thus making the sulfate oxygen unavailable for reaction with adsorbed *o*-DCB.

Bands similar to those discussed earlier also were seen in the case of Pd/Co–SZ (Figs. 9 and 10). However, during the adsorption of *o*-DCB on this sample at 250 °C, the band at 1532 cm^{-1} clearly split into two bands at 1574 and 1538 cm^{-1} (Fig. 9, traces a–c). This split could suggest acetate coordination on two different types of acid sites associated with Pd and SZ. Alternatively, such a split also could result from coupling between two C=O groups, indicating the presence of two bonds with predominantly a C=O

character in a surface oxalate species [37], favored in the presence of palladium.

A broad shoulder present at 1285 cm^{-1} (also seen on Co–SZ) can be assigned to the C–O stretching vibrations of the phenolate- or catecholate-type species formed after nucleophilic substitution on different sites. The intensity of this band was greater in the spectra of the Pd-containing samples, indicating greater activity. One interesting trend revealed by our data is that when Pd/Co–SZ was exposed to 8% O_2/He, the bands at 1348 and 1285 cm^{-1} increased in intensity, whereas the band at 1669 cm^{-1} almost disappeared (Fig. 9, traces f and g). Once again, this suggests the formation of phenolate- or catecholate-type species after nucleophilic substitution of the *o*-DCB coordinated on Lewis acid sites. Oxidation of such catecholate and/or phenolate resulted in formation of the carboxylates seen here [5,38]. Surface-bound phenolates and catecholates are commonly formed during the catalytic oxidation of 1,2-dichlorobenzene over V_2O_5/TiO_2 and V_2O_5/Al_2O_3 catalysts [4,5], the photocatalytic degradation of dihydroxybenzenes on Cu–TiO_2 [38], and the chemisorption of 2-chlorophenol on silica [39]. Alderman and Dellinger [39] found that 2-chlorophenol chemisorbed on silica at isolated and geminal surface hydroxyl groups to form surface-bound 2-chlorophenolate and catecholate species, respectively. Araña et al. [38] further demonstrated that the presence of a second metal [e.g., example Cu (II) on the TiO_2 surface] modified the surface catalytic centers. Thus, surface hydroxyl groups associated with each metal could favor the formation of different intermediates (i.e., phenolates and catecholates). In our case, it appears that catecholate species were formed in the presence of Co and Pd. It is interesting that the band at 1669 cm^{-1} disappeared in a stream of 8% O_2/He (Fig. 9, traces f and g), whereas the bands assigned to oxygenate species became more pronounced. This finding suggests that the adsorbed *o*-DCB species associated with the band at 1669 cm^{-1} was a precursor to these partially oxidized products. Furthermore, oxidation of the surface phenolates and carboxylates was slower than those of the adsorbed *o*-DCB precursor.

Under reaction conditions, the spectra of the Pd/Co–SZ samples (Fig. 10) included bands similar to those seen during *o*-DCB adsorption. But the presence of palladium appears to have facilitated oxidation to acetates, as indicated by the greater intensities of the corresponding bands compared with the spectra of SZ (Fig. 4) and Co–SZ (Fig. 7). Most likely, the PdO particles present on this catalyst were responsible for this enhanced oxidation activity. In agreement with previous reports [5,9,16], removing oxygen from the metal oxide is a kinetically significant step in the reaction mechanism and appears to be facilitated in the presence of Pd. A similar concerted reaction mechanism was reported previously for other oxide catalysts [5,16,19], involving Lewis acid sites located near an oxide or hydroxide nucleophilic site and leading to nucleophilic substitution of the chlorine atom.

The differences in the behavior of SZ, Co–SZ, and Pd/Co–SZ catalysts can be attributed to the nature and stability of the species formed between Co and S. In the case of Co–SZ, nucleophilic oxygen involved in the reactive adsorption of *o*-DCB did not appear to be present in abundance on the catalyst surface. Our findings suggest that the impregnation of Pd on Co–SZ generated new sites involved in the *o*-DCB reaction. Catalytic activity measurements conducted in parallel [36] have indicated that both Co–SZ and Pd/Co–SZ are very stable catalysts for *o*-DCB reaction oxidation, but the presence of Pd increases the activity considerably, consistent with the concept of generation of new active sites.

3.3. Reaction mechanism

Despite the similarities seen in the spectra of ZrO_2 and SZ, the SZ exhibited greater intensities and better-defined bands. This suggests that the oxidation of *o*-DCB occurred over both catalysts through a similar pathway, although the reaction was enhanced over SZ catalysts. The catalytic oxidation of Cl–VOCs over supported metal systems is known to be affected by both basic (OH^- and O^{2-}) and Lewis acid sites [19] present on a zirconia support promoted with oxoanions, such as sulfates [12]. In fact, the presence of sulfates generates additional active centers. Furthermore, promotion with secondary phases may result in better control of the nature of the acid sites and the stability of the catalysts.

In the present study, partial oxidation products were seen in both the presence and absence of gas-phase oxygen, indicating involvement of surface oxygen in the oxidation process, as was reported earlier for other oxide catalysts [5,16]. Different types of oxygen species can be present on the surface of transition metal oxides. The roles of these adsorbed oxygen species on the catalytic oxidation of organic compounds have been explored extensively [40,41]. Electrophilic oxygen species with different stabilities and chemical reactivity are associated with molecularly adsorbed O_2 and partially reduced oxygen species, such O^{2-}, O_2^{2-}, and O^-. In contrast, O^{2-} lattice oxide ions are considered nucleophilic reactants [40]. Furthermore, two hydroxide species, S–OH and Zr–OH, are present on the surface of sulfated zirconia, as indicated by our FTIR results. These species can react with adsorbed *o*-DCB to form the surface acetates observed in the presence of either surface or gas-phase oxygen. Our findings further suggest that the presence of PdO on Co–SZ generates additional nucleophilic sites, and that easier surface oxygen removal may contribute to the reaction. This supports the idea that the surface intermediate characterized by the band at 1669 cm^{-1} is formed during the interaction of *o*-DCB with common Lewis acid sites present in all of the catalysts evaluated (i.e., SZ, Co–SZ, and Pd/Co–SZ), followed by a nucleophilic substitution of chlorine atoms. Finally, further oxidation to oxygenate species occurs. Some of the partial oxidation products formed on the surface can further react to form gas-phase reaction products (i.e., HCl, CO, CO_2, and H_2O) seen during *ortho*-dichlorobenzene oxidation over SZ, Co–SZ, and Pd/Co–SZ [36]. In general, under the conditions studied in this work, we found no characteristic bands associated with coke formation [42].

4. Conclusion

FTIR spectra collected during the adsorption and oxidation of *o*-DCB on SZ, Co–SZ, and Pd/Co–SZ indicate that similar surface species were formed on these catalysts, suggesting a common reaction mechanism. The reaction pathway includes the following steps: (1) molecular adsorption of *o*-DCB on Lewis acid sites; (2) nucleophilic substitution of the chlorine atoms, resulting in the formation of surface phenolate and catecholate species; and (3) reaction through electrophilic substitution with bond-breaking of the aromatic ring to produce partial oxidation products. Our findings further indicate that surface oxygen, acting as a nucleophile, is involved in the oxidation process. The availability and activity of such oxygen species is affected by the interactions among surface sulfates, cobalt, and palladium, leading to differences in the catalytic behavior of the materials evaluated.

Acknowledgments

This work was supported by Universidad de Antioquia, through project CODI MDC04-1-01. B.H. Aristizábal thanks Colciencias for a doctoral fellowship and the catalysis group at the University of South Carolina for their hospitality and support during her stay.

References

[1] G. McKay, Chem. Eng. J. 86 (2002) 343.

[2] H.L. Tidahy, S. Siffert, J.-F. Lamonier, E.A. Zhilinskaya, A. Aboukaïs, Z.-Y. Yuan, A. Vantomme, B.-L. Su, X. Canet, G. De Weireld, M. Frère, T.B. N'Guyen, J.-M. Giraudon, G. Leclercq, Appl. Catal. A 310 (2006) 61.
[3] A. Predoeva, S. Damyanova, E.M. Gaigneaux, L. Petrov, Appl. Catal. A 319 (2007) 14.
[4] S. Krishnamoorthy, M.D. Amiridis, Catal. Today 51 (1999) 203.
[5] J. Lichtenberger, M.D. Amiridis, J. Catal. 223 (2004) 296.
[6] F. Bertinchamps, C. Grégoire, E.M. Gaigneaux, Appl. Catal. B 66 (2006) 1.
[7] F. Bertinchamps, C. Grégoire, E.M. Gaigneaux, Appl. Catal. 66 (2006) 10.
[8] F. Bertinchamps, A. Attianese, M.M. Mestdagh, E.M. Gaigneaux, Catal. Today 112 (2006) 165.
[9] F. Wyrwalski, J.-F. Lamonier, S. Siffert, A. Aboukaïs, Appl. Catal. B 70 (2007) 393.
[10] M. Labaki, S. Siffert, J.-F. Lamonier, E. Zhilinskaya, A. Aboukaïs, Appl. Catal. B 43 (2003) 261.
[11] A. Hofmann, J.J. Sauer, Phys. Chem. B 108 (2004) 14652.
[12] A. Corma, H. García, Catal. Today 38 (1997) 257.
[13] V. Adeeva, J.W. de Haan, J. Janchen, G.D. Lei, V. Schunemann, L.J.M. van de Ven, W.M.H. Sachtler, R.A. van Santen, J. Catal. 151 (1995) 364.
[14] M. Kantcheva, A.S. Vakkasoglu, J. Catal. 223 (2004) 352.
[15] L.F. Cordoba, W.M.H. Sachtler, C. Montes de Correa, Appl. Catal. B 56 (2005) 269.
[16] M.A. Larrubia, G. Busca, Appl. Catal. B 39 (2002) 343.
[17] M. Nagao, Y. Suda, Langmuir 5 (1989) 42.
[18] P. Davit, G. Martra, S.J. Coluccia, Jpn. Petrol. Inst. 47 (2004) 359.
[19] Q. Dai, G.N. Robinson, A. Freedman, J. Phys. Chem. B 101 (1997) 4940.
[20] M. Kantcheva, E.Z. Ciftlikli, J. Phys. Chem. B 106 (2002) 3941.
[21] P.S. Chintawar, H.L. Greene, J. Catal. 165 (1997) 12.
[22] S.T. Korhonen, S.M.K. Airaksinen, A.O.I. Krause, Catal. Today 112 (2006) 37.
[23] K. Föttinger, G. Kinger, H. Vinek, Appl. Catal. A 266 (2004) 195.
[24] D. Carmello, E. Finocchio, A. Marsella, B. Cremaschi, G. Leofanti, M. Padovan, G. Busca, J. Catal. 191 (2000) 354.
[25] B.H. Aristizábal, C. Montes de Correa, A.I. Serykh, C.E. Hetrick, M.D. Amiridis, Microporous Mesoporous Mater. 112 (2008) 432.
[26] P.A. Carlsson, L. Österlund, P. Thormählen, A. Palmqvist, E. Fridell, J. Jansson, M. Skoglundh, J. Catal. 226 (2004) 422.
[27] M.I. Zaki, M.A. Hasan, L. Pasupulety, Langmuir 17 (2001) 768.
[28] R.W. Stevens Jr., S.S.C. Chuang, B.H. Davis, Appl. Catal. A 252 (2003) 57.
[29] X. Li, K. Nagaoka, J.A. Lercher, J. Catal. 227 (2004) 130.
[30] C. Morterra, G. Cerrato, F. Pinna, M. Signoretto, J. Catal. 157 (1995) 109.
[31] D.A. Ward, E.I. Ko, J. Catal. 157 (1995) 321.
[32] C. Morterra, G. Cerrato, C. Emanuel, V. Bolis, J. Catal. 142 (1993) 349.
[33] J.A. Moreno, G. Poncelet, J. Catal. 203 (2001) 453.
[34] M.R. Gonzalez, K.V. Fogash, J.M. Kobe, J.A. Dumesic, Catal. Today 33 (1997) 303.
[35] X. Li, K. Nagaoka, L.J. Simon, J.A. Lercher, S. Wrabetz, F.C. Jentoft, C. Breitkopf, S. Matysik, H. Papp, J. Catal. 230 (2005) 214.
[36] B.H. Aristizábal, C. Maya, C. Montes de Correa, Appl. Catal. A 335 (2008) 211.
[37] S.J. Hug, B. Sulzberger, Langmuir 10 (1994) 3587.
[38] J. Araña, C. Fernández-Rodríguez, O. González-Díaz, J.A. Herrera-Melián, J. Pérez-Peña, Catal. Today 101 (2005) 261.
[39] S.L. Alderman, B. Dellinger, J. Phys. Chem. A 109 (2005) 7725.
[40] G. Busca, Catal. Today 27 (1996) 457.
[41] V.V. Kaichev, V.I. Bukhtiyarov, M. Hävecker, A. Knop-Gercke, R.W. Mayer, R. Schlögl, Kinet. Catal. 44 (2003) 432.
[42] B. Li, R.D. González, Appl. Catal. A 174 (1998) 109.